Published in final edited form as:
Environ Sci Technol. 2009 April 1; 43(7): 2581–2588.

UVA/B-Induced Formation of Free Radicals from Decabromodiphenyl Ether (Deca-BDE)

Yang-won Suh[†], **Garry R. Buettner**[Φ,‡], **Sujatha Venkataraman**[‡], **Stephen E. Treimer**[§], **Larry W. Robertson**[†,Φ], and **Gabriele Ludewig**[†,Φ,*]

† *Department of Occupational and Environmental Health, The University of Iowa, Iowa City, IA 52242, USA*

Φ *Interdisciplinary Graduate Program in Human Toxicology, The University of Iowa, Iowa City, IA 52242, USA*

‡ *Free Radical and Radiation Biology Program, ESR Facility, The University of Iowa, Iowa City, IA 52242, USA*

§ *Hygienic Laboratory, The University of Iowa, Iowa City, IA 52242, USA*

Abstract

Polybrominated diphenyl ether (PBDE) flame retardants are ubiquitous in the environment and in humans. A decabromodiphenyl ether mixture (deca-BDE) is the dominating commercial PBDE product today. Deca-BDE is degraded by UV to PBDEs with fewer bromines. We hypothesized that photodegradation of deca-BDE results in the formation of free radicals. We employed electron paramagnetic resonance (EPR) with spin trap agents to examine the free radicals formed from UV irradiation of a deca-BDE mixture (DE-83R). The activating wavelength for deca-BDE photochemistry was in the UVA to UVB range. The yields of radicals from irradiated deca-BDE in tetrahydrofuran (THF), dimethylformamide (DMF), and toluene were about 9-, 4-, and 7-fold higher, respectively, than from irradiated solvent alone. Radical formation increased with deca-BDE concentration and irradiation time. The quantum yield of radical formation of the deca-BDE mixture was higher than with an octa-BDE mixture (DE-79; ~2-fold), decabromobiphenyl (PBB 209; ~2-fold), decachlorobiphenyl (PCB 209; ~3-fold), and diphenylether (DE; ~6-fold), indicating the positive effects of bromine and an ether bond on radical formation. Analysis of hyperfine splittings of the spin adducts suggests that radical formation is initiated or significantly enhanced by debromination paired with hydrogen abstraction from the solvents. To our knowledge this is the first report that uses EPR to demonstrate the formation of free radicals during the photolytic degradation of PBDEs. Our findings strongly suggest the potential of negative consequences due to radical formation during UV exposure of PBDEs in biological systems.

Introduction

The flame retardants polybrominated diphenyl ethers (PBDEs) are a global environmental issue because of their ubiquitous presence in human blood, breast milk and tissues, in our indoor and outdoor environment, and in ecosystems (1,2). PBDEs, widely used in diverse products including electronic equipment, furniture, and textiles, are commercially produced and used as penta-, octa-, and decabrominated diphenyl ether (BDE) mixtures, named in this way to

*Corresponding author address: Department of Occupational & Environmental Health, College of Public Health, University of Iowa, 100 Oakdale Campus, #234 IREH, Iowa City, IA 52242-5000; phone: 319-335-4650; fax 319-335-4290; e-mail: E-mail: gabriele-ludewig@uiowa.edu.

Supporting Information Available. Two tables, seven figures, four paragraphs._This information is available free of charge via the Internet at http://pubs.acs.org.

indicate the average number of bromines on the diphenyl ether core structure (1,2). They are structurally similar to the polyhalogenated biphenyls (PBBs and PCBs) and, like them are highly lipophilic and bioaccumulate. The adverse effects of PBDEs on human and animal health have not been adequately studied, however, indications of neurotoxicity, thyroid hormone disruption, and, for deca-BDE, carcinogenicity have been observed (1–3).

PCBs and PBBs are known to undergo photolytic dehalogenation to lower halogenated biphenyls, and may form dibenzofurans, and other by-products from secondary and tertiary reactions (4–8). Similarly PBDEs in pure solvents (acetonitrile, ethanol, methanol, hexane, THF, and toluene), aqueous solutions, sediment and other media were shown to photolytically degrade to products that are more toxic and more bioavailable (9–16). In these matrices, PBDEs absorbed UVC (250 – 280 nm), UVB (280 – 320 nm) and part of UVA (320 – 350 nm) from artificial UV light sources or natural solar light and degraded to lower BDEs and other compounds, including polybrominated dibenzofurans (PBDFs), brominated 2-hydroxybiphenyls and bromobenzene (9,11,14,17). Using light intensities in the range of natural solar light, this required exposure times of only minutes to weeks. It has been hypothesized that free radical processes are involved in the photodegradation *via* light-induced homolytic breakage of aryl-Br and/or ether bonds of PBDEs, thereby generating aryl and bromine radicals (16–18).

Recent studies reported very high levels of PBDEs in indoor dust of US houses (8.2 μg/g) and houses and cars in Great Britain (260 and 340 μg/g dust, respectively) (3,19), with deca-BDE as the dominant congener. PBDEs are used as additives, i.e. not covalently bound to the polymers, and therefore easily released from the consumer product into the air and house dust (20). As a consequence, dermal contact with PBDEs in dust may contribute more to the body burden than food intake and inhalation, which is in contrast to other halogenated organic compounds (3). Remarkably, dermal exposure to halogenated compounds plus UV light may potentiate the risk of toxic effects, most likely due to radical formation. UV irradiation of patients treated with potassium bromide resulted in severe skin ulceration and necrosis (21). Linemen and cable splicers, typical outdoor occupations, had significantly higher risk for melanoma after long term dermal exposure to PCBs (22). While PBDE levels on human skin have not yet been thoroughly investigated, a recent analysis found PBDE concentrations normalized to skin surface area in the range of 3 – 1970 pg/cm^2 (23). The backside of a young male hand secretes about 38 μg/cm^2 of surface skin lipids over 3 h (24). Based on this, we assume that the PBDE levels in skin surface lipid may be in the range of 0.1 – 50 μg/g lipid. In daily life skin is exposed to UV light. It required only 2 min of exposure to sunlight to degrade over 20% of hepta-BDE dissolved in lipids (BDE-183; 25 ng/g lipid) (25). Thus, the amount and the reactivity of deca-BDE on the skin surface could be high enough to induce a photochemical reaction and toxicity and UV-induced radical formation of PBDEs should be carefully investigated.

We hypothesized that irradiation of deca-BDE produces free radicals which can be detected and identified by electron paramagnetic resonance (EPR) spectrometry, the only direct method to detect and identify free radicals. We investigated the relationships of free radical formation upon exposure to UV light to: concentration of deca-BDE, irradiation time, and structure of various halogenated compounds or mixtures, i.e. DE-83R (deca-BDE mixture), DE-79 (octa-BDE mixture), decabromobiphenyl (PBB 209), decachlorobiphenyl (PCB 209), and diphenyl ether (DE), and analyzed the mechanisms of radical formation.

Materials and Methods

Chemicals

The commercial deca-BDE mixture DE-83R (>98% BDE-209) and the octa-BDE mixture DE-79 (containing BDE-209 (<0.70%), nona-BDEs (<10%), octa-BDEs (<33%), hepta-BDEs (<45%), hexa-BDEs (<12%), penta-BDEs (<0.50%)) are a gift from Great Lakes Chemical Co. (West Lafayette, U.S.A.). In this paper, the term deca-BDE and octa-BDE indicate DE-83R and DE-79, respectively. BDE-209 indicates the deca-BDE congener. Decabromobiphenyl (PBB 209) and decachlorobiphenyl (PCB 209) were purchased from Accustandard Inc. (New Haven, U.S.A.). 5,5-Dimethylpyrroline-N-oxide (DMPO) was from Dojindo (Gaitherburg, MD) and 2-methyl-2-nitrosopropane (MNP) was from Sigma (St. Louis, U.S.A.). DE, THF with butylated hydroxytoluene (BHT), deuterated THF (THF-d8) without BHT and DMF were from Acros (New Jersey, U.S.A.). THF without BHT and toluene were from Burdick & Jackson (Muskegon, MI, U.S.A.). THF was selected as a solvent because it has been used in previous photodegradation studies of PBDEs due to its very good solvent activity compared to other solvents and known to be a good hydrogen donor, which facilitates debromination of PBDEs (10). DMF and toluene were included as solvents for deca-BDE to study solvent effects on the radical formation. The structures of chemicals are depicted in Supporting Information (Tables S1 and S2).

EPR

A Bruker EMX EPR spectrometer (Karlsruhe, Germany) equipped with a 4103TM cavity was used. Typical instrument settings were: microwave frequency, 9.8 GHz (X-band); microwave power, 20 mW; modulation amplitude, 1.0 G; time constant, 0.2 s; scan rate, 80 G/84 s; receiver gain, 2×10^2–3×10^4. Test compounds were dissolved in the appropriate solvent. Spin traps were added to obtain a final concentration of 25 mM DMPO (from a 1 M aqueous stock) or 10 mM MNP (prepared in the dark). Estimates of absolute concentrations of spin adduct were accomplished by double integration of spectra and comparison to a standard of 3-carboxyproxyl (3-CxP) using the same instrument settings and physical setup (26). Simulation of EPR data was accomplished using WinSim software (NIEHS) and Bruker WinEPR (Karlsruhe, Germany). The Spin Trap Database (NIEHS) was referred to interpret and simulate EPR spectra (27). Simulated spectra correlated well with corresponding experimental spectra (correlation coefficient >0.99).

Irradiation

A 150 W Photomax Xenon arc lamp (Oriel, Stratford, CT, USA) was used to irradiate samples. The power of the lamp was set at 30 W. All samples were irradiated at room temperature for 14 minutes and with DMPO, unless otherwise indicated. A 309 (WG 305), 280 (WG 280) or 400 nm (BG 12) cut-off filter (cutting off the shorter wavelengths; specification: 50% transmittance at 309, 280 or 400 nm, respectively) from Schott (Duryea, PA, USA) was inserted into the lamp to minimize the photodegradation of spin traps and solvents at shorter wavelengths. Since oxygen broadens the EPR lines thus lowering the resolution, samples were bubbled with argon to partially remove oxygen and then transferred to a flat quartz cell. The path length for UV irradiation of the flat cell was 0.3 mm. The cell was placed into the TM cavity and the sample was irradiated (Xenon lamp at ~50 cm distance) while in the EPR cavity. For photodegradation studies, samples in a standard 1 cm quartz cuvette were exposed to light from the Xenon lamp with a 309 nm cut-off filter. An IL1400 BL radiometer with UV GAL.NIT detector from International Light Inc. (Peabody, MA, U.S.A.) was used to measure the light intensity. The light intensity was 2.3 and 3.5 mW/cm^2 with the 309 and 280 nm filter, respectively, for both the EPR and cuvette photodegradation studies.

GC-MS and Absorption spectra

See Supporting Information.

Results and Discussion

Radical formation by irradiation of deca-BDE

EPR spin trapping experiments with DMPO demonstrate that high levels of free radicals are produced during irradiation of deca-BDE (Figure 1). Irradiation of solvent alone produces much weaker background EPR signals (Figure 1 spectra b and c of each panel). The radical yields from deca-BDE in THF, DMF, and toluene were about 9-, 4-, and 7-fold higher than from solvent alone, respectively, indicating that deca-BDE is directly involved in increased radical formation. Previous studies have suggested that the hydrogen-donating ability of a solvent significantly affects the rate of photodegradation of PBDE (16). This is in agreement with our observation that THF, which is a good hydrogen-donor, facilitates the spin adduct formation more than the other solvents. The EPR spectra of the DMPO spin adducts formed during deca-BDE irradiation show different spectral features in each of the three organic solvents used (THF, Figure 1A-a; DMF, B-a; toluene, C-a). This suggests that the different spin adducts arise because of the different solvents, not from the BDE. The concentrations of deca-BDE used were 2 mM in THF and DMF, and 1 mM in toluene while the concentration of solvent is ≈10 M and that of DMPO only 25 mM. Thus, oxidants produced by the interaction of BDE and light will kinetically have the highest probability of reacting with solvent; the resulting solvent-derived radicals will in turn be trapped by DMPO. A general mechanism in agreement with these observations is:

$$\text{Deca} - \text{BDE} + h\nu \rightarrow \text{nona} - \text{BDE}^{\bullet} + \text{Br}^{\bullet} \quad (1)$$

$$\text{nona} - \text{BDE}^{\bullet} + \text{Solvent} \rightarrow \text{Solvent}^{\bullet} + \text{nona} - \text{BDE} \quad (2)$$

$$\text{Br}^{\bullet} + \text{Solvent} \rightarrow \text{Solvent}^{\bullet} + \text{HBr} \quad (3)$$

$$\text{Solvent}^{\bullet} + \text{DMPO} \rightarrow \text{DMPO/Solvent}^{\bullet} \quad (4)$$

Photodegradation of deca-BDE

When 0.5 mM deca-BDE in toluene was exposed to UV light (1 cm quartz cuvette with a 309 nm cutoff filter) a loss of BDE-209 was observed with a concomitant formation of degradation products (Figure S2-A). This loss of BDE-209 and formation of photoproducts increased with time of exposure. Three nona-BDE congeners (BDE-206, 207, and 208) and an octa-BDE congener (BDE-203) were identified. The lag-time required before the octa-BDE congeners appear suggest that these degradation products were derived from the newly formed nona-BDE congeners. This is in agreement with previous reports (10–13). One unknown peak close to the octa-BDE congeners was observed (Figure S2-B), probably a hexabromodibenzofuran (hexa-BDF) congener considering its retention time and mass data.

Spin adduct formation increases with irradiation time and concentration of deca-BDE

The total amount of spin adducts formed increased with irradiation time (309 nm cut-off) for all solvents (Figure S3-A) and with concentration of deca-BDE in THF and DMF (Figure S3-

B). With either increase in time-of-exposure or concentration of deca-BDE an apparent steady-state level of spin adducts is approached or attained, consistent with both formation and expected loss of spin adduct. The solvent-only derived spin adduct barely changed with exposure time (data not shown). Thus, deca-BDE presence was essential for strong spin adduct generation.

The formation of deca-BDE-derived spin adducts requires UV light of wavelengths <400 nm

When a 400 nm cut-off filter is used, only a very weak solvent radical spectrum is observed (Figure S4). Deca-BDE absorbs readily in the wavelength range passed by a 309 nm filter, but there is no absorbance above ~350 nm (Figure S1). THF, DMF, toluene, and DMPO (λ_{max} = 230 nm, $\varepsilon_{228} = 7.7 \times 10^3\ M^{-1}\ cm^{-1}$) (28) do not absorb significantly in this range (Figure S1). Thus, the activating wavelength for radical formation from deca-BDE is in the UVA (400-320 nm) to UVB (320-280 nm) range. The spectra of MNP monomer and dimer display maximum light absorption at 675 and 295 nm, respectively (29). This indicates that the 309 nm filter sufficiently shields the solvents, DMPO and MNP monomer from UV degradation, but allows the halogenated test compounds to react with the longer wavelength UV light.

Deca-BDE yields more radicals than related compounds

We investigated the radical yield of deca-BDE compared to similar organic compounds, i.e. octa-BDE, PBB 209, PCB 209, and DE. Irradiation of 1 mM solutions of each compound in THF, using a 309 nm cut-off filter, resulted in formation of the same DMPO spin adducts and similar spectral patterns, but the radical yields were very different (Figures 2-A and S5). The spin adduct yield from deca-BDE was ~2-fold higher than from octa-BDE and PBB 209, ~3-fold higher than PCB 209, and ~6-fold higher than DE or solvent alone. Use of a 280 nm cut-off filter resulted in a general increase in radical formation by maintaining the same order of compounds, although the increase was higher with the other halogenated compounds compared to deca-BDE. The UV absorption spectra show that deca-BDE absorbs at longer wavelengths than the other compounds (Figure S1) (10, 30); the actual quantum yields of degradation are quite similar (10). Additionally, the integrated UV spectra correlate positively with the radical yields (Figure 2-B-a/b). This demonstrates that the rate of degradation depends on the degree of UV absorption by the compound. Heat of formation (ΔH_f), bond dissociation energy, and energy of the highest occupied molecular orbital (E_{HOMO}) and lowest unoccupied molecular orbital (E_{LUMO}) have been used to predict degradation rates of PBDEs and PCBs during irradiation (31–34). Photodegradation rates of PBDEs increase with number of C-Br bonds (10). Thus, it is suggested that higher bromine content results in a smaller difference between E_{LUMO} and E_{HOMO} (dE) and higher ΔH_f, which in turn will result in a greater yield of free radicals (31). An inverse correlation was found between phototoxicity and dE of polycyclic aromatic hydrocarbons (PAHs) and suggested to be related to the ease of radical formation (35).

The EPR signal intensity from brominated biphenyl was clearly higher than of chlorinated biphenyl. A possible reason could be the red-shift in the spectrum of PBB compared to PCB as well as the lower bond dissociation energy of C-Br (331–343 kJ/mol) compared to C-Cl (~350–400 kJ/mol) in aryl halides (16,36), as proposed (37). The ether bridge in PBDE further increases the red shift, accompanied by an increased yield of radicals compared to PBB 209. This shows that PBDEs will be significantly more photoactive upon exposure to solar UV light than parallel chlorinated compounds and/or halogenated biphenyls.

DMPO Spin Adduct Identification

To assist in the identification of the observed spin adducts with DMPO we simulated key spectra (Figure 3). The weak solvent spectra, Figure 3-A-a (and Figures 1-A-b,c and S4) have the appearance and splitting constants consistent with the spin trapping of superoxide (or

hydroperoxyl radical HOO$^{\bullet}$) in an organic solvent (a^N = 13.0 G; a_β^H = 7.07 G; a_γ^H = 2.05 G, NoH) = 1.84) forming adduct A (Figure 5). (NoH is the ratio of the nitrogen hyperfine splitting to the hydrogen hyperfine splittings (NoH = a^N/a^H)) (27,38). Adduct B would be formed in the absence of oxygen. (for more details see Supporting Information).

The spectra obtained from deca-BDE with DMPO in THF are quite different from those of DMPO in THF alone. The presence of deca-BDE (2 mM) results in a much more intense spin adduct EPR signal than observed from THF alone, ≈25-fold more (Figure 3A/B-a). This spin adduct appears to be identical to adduct C derived from the carbon-centered radical IV in Figure 6 observed with THF alone (Figure 3A/B-e). Because neat THF is ≈10 M, and DMPO is only 25 mM, oxidants produced from photoexcited deca-BDE (Br$^{\bullet}$ and a BDE-carbon-centered radical (V)) will react preferentially with THF forming the THF radical and lower BDE, *e.g*. nona-BDE *via* hydrogen abstraction; DMPO will then trap solvent-derived radicals, producing adduct C (Figure 5). The EPR simulations indicate that the spectra obtained from irradiated solvent alone and from irradiating deca-BDE in THF share the same set of spin adducts, but in very different proportions. With THF alone, DMPO/$^{\bullet}$OR and DMPO/$^{\bullet}$OOH are dominant (A + B = >98% of total adducts), while light exposure of deca-BDE produced predominantly the DMPO/$^{\bullet}$tetrahydrofuranyl spin adduct (C), increasing this adduct from 1.6% to >86% of all adducts.

Spin Trapping with MNP

Because DMPO does not typically demonstrate observable hyperfine splittings from nuclei on the trapped radical, we used MNP, a nitroso spin trap to learn more about the carbon-centered radicals trapped by DMPO. The disadvantage of MNP is that oxygen-centered spin adducts are very short-lived and thus not observable in steady-state experiments; in addition, the photolytic cleavage (at the wavelengths used) of the C-N nitroso bond, produces a *tert*-butyl radical which will be trapped by MNP thus forming the di-*tert*-butylnitroxide (DTBN, MNP/*tert*-butyl$^{\bullet}$) with a simple 1:1:1 triplet spectrum (Figure 5, E) (29). As expected, all MNP samples contained varying levels of the triplet spectrum which increased with irradiation (Figure 4, S6 and S7). The presence of deca-BDEweakened the triplet spectrum from DTBN (Figure 4A-a/b-1 and Figure 4B-a/b-1), most likely due to significant light absorption by deca-BDE, thereby limiting the photochemistry for its formation. Alternatively, since the intensity of DTBN is pH dependent (29), the effect could be due to production of HBr from irradiation of deca-BDE, which dissociates to H^+ and Br^-, thereby decreasing the pH. Irradiation of deca-BDE in THF or toluene in the presence of MNP produced four additional peaks in the EPR spectra with peak intensity ratios of approximately 1:2:2:1 (Figure 4-A/B-a/a′). This spectral pattern is consistent with the hydrogen (or e^-_{aq}, H^+) spin adduct of MNP (MNP/H$^{\bullet}$) (27, 38). Simulation of experimental spectra yielded hyperfine splitting constants: MNP/*tert*-butyl$^{\bullet}$ (a^N = 15.30 G and 15.34 G in THF and toluene, respectively) and MNP/H$^{\bullet}$ (a^N = 14.87 G and a^H = 14.72 G) in both solvents (Figure S6A/B) (27, 38). These results suggest that a low yield of photoionization products (solvated electron and aryl radical cation) may be produced from irradiation of deca-BDE.

To gather evidence for our suggestion of MNP/H$^{\bullet}$ spin adducts as product of deca-BDE irradiation in THF we used THF-d8 in which all hydrogen atoms are replaced with deuterium atoms. The expected MNP/D$^{\bullet}$ spectrum should be quite different than MNP/H$^{\bullet}$ because of the different nuclear spins for deuterium (I = 1) and hydrogen (I = 0.5); in addition the nuclear magneton for deuterium is about 15% of that of hydrogen. Indeed, after irradiation of deca-BDE in THF-d8, the typical EPR peaks of an MNP-hydrogen adduct were basically absent (Figure S6 and S7-B-1/2), thus supporting our hypothesis that the hydrogen radical was derived from the solvent. However, at our signal-to-noise level the expected weak triplet of triplets signal was not observed, rather a new simple 1:1:1 species appeared along with DTBN.

Simulation of experimental spectra yielded hyperfine splitting constants: MNP/*tert*-butyl$^{\bullet}$ (a^N = 15.38) and MNP/D$^{\bullet}$ (a^N = 13.94 G and a^D = 0.34 G) (Figure S6-C). The addition of solvent protons by inclusion of water (THF-d8:water = 9:1) resulted in no change in the species observed, only in the ratio (Figure S6-D). These results suggest that the organic solvent is the main source for hydrogen radicals. While most nona-BDEs are expected to be further degraded to lower-BDEs (Figure 5, path 1) a certain amount of excited nona-BDE could react with MNP (path 2) and produce the MNP/H$^{\bullet}$ spin adducts (D) *via* reduction of MNP by electron transfer from the exited state of nona-BDE. If photoionization was a significant process, we would have also expected to see the MNP/H$^{\bullet}$ in THF-d8 + water (39, 40). This was not observed (Figure S6-D). Thus, if photoionization does occur it appears to be a minor process. MNP should capture carbon-centered radicals such as aryl radicals from deca-BDE more effectively than DMPO. The spin adducts of carbon-centered radicals, however, were not definitively observed, probably because the concentration of spin adducts of DTBN was very high and the hyperfine splittings of DTBN are very similar to the splittings of the radicals we were interested in (41). We were not able to detect the splittings of bromine radicals either, probably, as has been suggested earlier (42), because the hyperfine splittings of bromine with certain radicals are too small to be detected due to quadrupolar interruption.

Radical formation pathways and their implications

Reductive debromination is probably the main mechanism of photodegradation of PBDEs (15–18,43). It has been suggested that the homolytic dissociation of aryl-Br bonds leads to the debromination of PBDEs generating aryl and bromine radicals and subsequently lower brominated DEs, PBDFs and other degradation products (18,43). The aryl radicals are then proposed to abstract hydrogen atoms from their matrices thereby completing the reductive debromination process (16,18,43). The analysis of photodegradation products of irradiated BDE 15 (4,4′-dibromodiphenyl ether) suggested homolytic cleavage of C-Br as a dominant process since no O-aryl bond breakage products were formed, probably because the Br-aryl bond dissociation energy (~335 kJ/mol) is weaker than the O-aryl bond dissociation energy (~335–390 kJ/mol) (16,36). Other researchers suggest that photodegradation of PBDEs involve also aryl-oxygen bond cleavage with the generation of phenoxyl and aryl radicals (17,18). We did not detect clear evidence of products of ether bridge cleavage in our GS/MS analysis; however, they may have been below the detection limit after this short term exposure.

Our results with MNP show that irradiation of deca-BDE in THF and toluene produces hydrogen atom spin adducts and that the hydrogen radicals are from the solvents. Simulation data from experiments with DMPO suggest that irradiation of deca-BDE led to the formation of solvent radicals *via* hydrogen abstraction. Thus the primary mechanism of radical formation during PBDE photodegradation in solvents is hydrogen abstraction from matrices, a secondary event following the debromination process of PBDEs *via* homolytic cleavage of C-Br (Figure 5). This hydrogen abstraction deserves special attention, since in biological systems, hydrogen abstraction initiates lipid and protein oxidation, thereby producing various radicals and electrophiles which may attack critical cellular macromolecules, including the DNA. For example, irradiation of chloropromazine produced radicals that homolytically changed sulfhydryl or peptide bonds *via* hydrogen abstraction (44). The human skin surface is covered with lipids whose unsaturated bonds are subjected to hydrogen abstraction by free radicals. Polyunsaturated fatty acids (PUFA) in surface skin lipids could be more easily involved in hydrogen abstraction than THF because PUFA's bond energy (75–80 kcal/mol at allylic position) is lower than the dissociation energy of α-carbon bond of THF (92 kcal/mol) (45, 46). Indeed, PBDEs in lipid degrade quickly if exposed to sunlight (25). Irradiation of halogenated PAHs in lipids significantly increased lipid peroxides (47). Peroxidation of skin surface lipids deteriorates membrane function (48). Lipid peroxides from surface skin lipids lead to cell damage in keratinocytes and stimulated cell growth and altered epidermal structure

in skin tissues (49). Therefore, our observation of UV-induced radical formation of PBDEs in THF *via* hydrogen abstraction from its solvent suggests that PBDEs could also be photoreactive and phototoxic on human skin. Radical formation could also occur in skin tissue, since lower brominated BDEs easily penetrate into the skin (50) and may reach the skin after internal uptake (51). UV A and B penetrate the stratum corneum and can lead to cancer in the stratum germinativum. Dermal PCB exposure has been shown to significantly increase the risk of melanoma in linemen, cable splicers and electricians (22). This risk was considered so substantial that NIOSH issued a warning for melanoma risk in these workers (52) who are co-exposed to UV light, since they are working frequently outdoors (22). PBDEs may be an even greater risk factor, due to the widespread contamination levels and - as shown in this study - significantly stronger activity in radical formation compared to PCBs. Young children may be at particularly high risk, since they have generally higher PBDE contamination levels than adults (53), more outdoor activity and therefore UV exposure, and higher risk of percutaneous toxicity due to their specific skin structure (54). This potential risk of skin damage and carcinogenesis by radical formation due to UV-exposure of PBDEs needs urgent clarification.

We demonstrated radical formation by irradiation of deca-BDE with UV-A/B light and we could show that the type of halogen, *i.e.* Br > Cl, a higher number of halogens in the molecule, and the ether bridge between the phenyl rings all strongly favor radical formation by deca-BDE. This is important new information, since it indicates that deca-BDE may have a so far unrecognized, significant mechanism of toxicity. Thus, light exposure of deca-BDE in the skin, may cause serious toxic effects, even carcinogenicity. Therefore additional studies of the consequences of UV irradiation of deca-BDE in biological systems are urgently needed.

Supplementary Material

Refer to Web version on PubMed Central for supplementary material.

Acknowledgments

Acknowledgements. The project described was supported by NIEHS P42 ES013661, DOD DAMD17-02-1-0241, EPA R-82902102-0, CHEEC, and NIGMS R01 GM073929. The contents are solely the responsibility of the authors and do not necessarily represent the official views of these funding agencies. The University of Iowa ESR Facility provided invaluable support; we thank Brett Wagner and Karl Niggemeyer for their assistance.

Literature Cited

1. Vonderheide AP, Mueller KE, Meija J, Welsh GL. Polybrominated diphenyl ethers: Causes for concern and knowledge gaps regarding environmental distribution, fate and toxicity. Sci Total Environ 2008;400(1–3):425–36. [PubMed: 18571221]
2. Ward J, Mohapatra SP, Mitchell A. An overview of policies for managing polybrominated diphenyl ethers (PBDEs) in the Great Lakes basin. Environ Int 2008;34(8):1148–56. [PubMed: 18579207]
3. Lorber M. Exposure of Americans to polybrominated diphenyl ethers. J Expo Sci Environ Epidemiol. 2007
4. Robertson LW, Chittim B, Safe SH, Mullin MD, Pochini CM. Photodecomposition of a commercial polybrominated biphenyl (PBB) fire retardant: High-resolution gas chromatographic analysis. J Agric Food Chem 1983;31(2):454–457.
5. Manzano MA, Perales JA, Sales D, Quiroga JM. Using solar and ultraviolet light to degrade PCBs in sand and transformer oils. Chemosphere 2004;57(7):645–654. [PubMed: 15488927]
6. Miao X-S, Chu S-G, Xu X-B. Degradation pathways of PCBs upon UV irradiation in hexane. Chemosphere 1999;39(10):1639–1650. [PubMed: 10520484]
7. von der Recke R, Vetter W. Photolytic transformation of polybrominated biphenyls leading to the structures of unknown hexa- to nonabromo-congeners. J Chromatogr A 2007;1167(2):184–194. [PubMed: 17825831]

8. Bunce NJ, Landers JP, Langshaw JA, Nakai JS. An assessment of the importance of direct solar degradation of some simple chlorinated benzenes and biphenyls in the vapor phase. Environ Sci Technol 1989;23(2):213–218.
9. Hagberg J, Olsman H, van Bavel B, Engwall M, Lindström G. Chemical and toxicological characterisation of PBDFs from photolytic decomposition of decaBDE in toluene. Environ Int 2006;32 (7):851–7. [PubMed: 16815548]
10. Eriksson J, Green N, Marsh G, Bergman A. Photochemical decomposition of 15 polybrominated diphenyl ether congeners in methanol/water. Environ Sci Technol 2004;38(11):3119–25. [PubMed: 15224744]
11. Söderström G, Sellström U, de Wit CA, Tysklind M. Photolytic debromination of decabromodiphenyl ether (BDE 209). Environ Sci Technol 2004;38(1):127–32. [PubMed: 14740727]
12. Ahn MY, Filley TR, Jafvert CT, Nies L, Hua I, Bezares-Cruz J. Photodegradation of decabromodiphenyl ether adsorbed onto clay minerals, metal oxides, and sediment. Environ Sci Technol 2006;40(1):215–20. [PubMed: 16433354]
13. Bezares-Cruz J, Jafvert CT, Hua I. Solar photodecomposition of decabromodiphenyl ether: products and quantum yield. Environ Sci Technol 2004;38(15):4149–56. [PubMed: 15352454]
14. Rayne S, Wan P, Ikonomou M. Photochemistry of a major commercial polybrominated diphenyl ether flame retardant congener: 2,2′,4,4′,5,5′-hexabromodiphenyl ether (BDE153). Environ Int 2006;32(5):575–85. [PubMed: 16581124]
15. Hua I, Kang N, Jafvert CT, Fabrega-Duque JR. Heterogeneous photochemical reactions of decabromodiphenyl ether. Environ Toxicol Chem 2003;22(4):798–804. [PubMed: 12685715]
16. Rayne S, Ikonomou MG, Whale MD. Anaerobic microbial and photochemical degradation of 4,4′-dibromodiphenyl ether. Water Res 2003;37(3):551–60. [PubMed: 12688689]
17. Watanabe I, Tatsukawa R. Formation of brominated dibenzofurans from the photolysis of flame retardant decabromobiphenyl ether in hexane solution by UV and sun light. Bull Environ Contam Toxicol 1987;39(6):953–9. [PubMed: 3440151]
18. Rayne S, Wan P, Ikonomou M. Photochemistry of a major commercial polybrominated diphenyl ether flame retardant congener: 2,2′,4,4′,5,5′-hexabromodiphenyl ether (BDE153). Environ Int 2006;32(5):575–85. [PubMed: 16581124]
19. Stuart H, Ibarra C, Abdallah MA-E, Boon R, Neels H, Covaci A. Concentrations of brominated flame retardants in dust from United Kingdom cars, homes, and offices: Causes of variability and implications for human exposure. Environ Int 2008;34(8):1170–1175. [PubMed: 18558431]
20. D'Silva K, Fernandes A, Rose M. Brominated organic micropollutants-igniting the flame retardant issue. Crit Rev Environ Sci Technol 2004;34:141–207.
21. Diener W, Sorni M, Ruile S, Rude P, Kruse R, Becker E, Bork K, Berg PA. Panniculitis due to potassium bromide. Brain Dev 1998;20(2):83–87. [PubMed: 9545177]
22. Loomis D, Browning SR, Schenck AP, Gregory E, Savitz DA. Cancer mortality among electric utility workers exposed to polychlorinated biphenyls. Occup Environ Med 1997;54(10):720–8. [PubMed: 9404319]
23. Stapleton HM, Kelly SM, Allen JG, McClean MD, Webster TF. Measurement of polybrominated diphenyl ethers on hand wipes: Estimating exposure from hand-to-mouth contact. Environ Sci Technol 2008;42(9):3329–3334. [PubMed: 18522114]
24. Rajka G. Surface lipid estimation on the back of the hands in atopic dermatitis. Arch Dermatol Forsch 1974;251(1):43–8. [PubMed: 4282013]
25. Peterman PH, Orazio CE. Sunlight photolysis of 39 mono-hepta PBDE congeners in lipid. Organohal Comp 2003;63:357–360.
26. Venkataraman S, Martin SM, Schafer FQ, Buettner GR. Detailed methods for the quantification of nitric oxide in aqueous solutions using either an oxygen monitor or EPR. Free Radic Biol Med 2000;29(6):580–5. [PubMed: 11025201]
27. Li ASW, Cummings KB, Roethling HP, Buettner GR, Chignell CF. A spin trapping data base implemented on the IBM PC/AT. J Magn Reson 1988;79:140–142.
28. Hall RD, Buettner GR, Chignell CF. The biphotonic photoionization of chlorpromazine during conventional flash photolysis: Spin trapping results with 5,5-dimethyl-1-pyrroline-N-oxide. Photochem Photobiol 1991;54(2):167–173. [PubMed: 1664109]

29. Makino K, Suzuki N, Moriya F, Rokushika S, Hatano H. A fundamental study on aqueous solutions of 2-methyl-2-nitrosopropane as a spin trap. Radiat Res 1981;86(2):294–310.
30. MacNeil JD, Safe S, Hutzinger O. The ultraviolet absorption spectra of some chlorinated biphenyls. Bull Environ Contam Toxicol 1976;15(1):66–77. [PubMed: 819070]
31. Hu J, Eriksson L, Bergman A, Jakobsson E, Kolehmainen E, Knuutinen J, Suontamo R, Wei X. Molecular orbital studies on brominated diphenyl ethers. Part II--reactivity and quantitative structure-activity (property) relationships. Chemosphere 2005;59(7):1043–57. [PubMed: 15823338]
32. Li X, Fang L, Huang J, Yu G. Photolysis of mono-through deca-chlorinated biphenyls by ultraviolet irradiation in n-hexane and quantitative structure-property relationship analysis. J Environ Sci (China) 2008;20(6):753–759. [PubMed: 18763572]
33. Zeng X, Simonich SLM, Robrock KR, Korytár P, Alvarez-Cohen L. Development and validation of a congener-specific photodegradation model for polybrominated diphenyl ethers. Environ Toxicol Chem 2008;27(12):2427–2435. [PubMed: 18613751]
34. Niu J, Shen Z, Yang Z, Long X, Yu G. Quantitative structure-property relationships on photodegradation of polybrominated diphenyl ethers. Chemosphere 2006;64(4):658–665. [PubMed: 16343592]
35. Mekenyan OG, Ankley GT, Veith GD, Call DJ. QSARs for photoinduced toxicity: I. Acute lethality of polycyclic aromatic hydrocarbons to Daphnia magna. Chemosphere 1994;28(3):567–582.
36. Schutt, L.; Bunce, NJ. Photohalogenation of aryl halides. In: Horspool, WM.; Lenci, F., editors. CRC Handbook of Organic Photochemistry and Photobiology. CRC Press; 2004. p. 38-1-38-12.
37. Alonso M, Casado S, Miranda C, Tarazona J, Navas J, Herradón B. Decabromobiphenyl (PBB-209) activates the aryl hydrocarbon receptor while decachlorobiphenyl (PCB-209) is inactive: Experimental evidence and computational rationalization of the different behavior of some halogenated biphenyls. Chem Res Toxicol 2008;21(3):643–658. [PubMed: 18311929]
38. Buettner GR. Spin trapping: ESR parameters of spin adducts. Free Radic Biol Med 1987;3(4):259–303. [PubMed: 2826304]
39. Moore DE, Sik RH, Bilski P, Chignell CF, Reszka KJ. Phototochemical sensitization by azathioprine and its metabolites. Part 3. A direct EPR and spin-trapping study of light-induced free radicals from 6-mercaptopurine and its oxidation products. Photochem Photobiol 1994;60(6):574–581. [PubMed: 7870762]
40. Mossoba MM, Makino K, Riesz P. Photoionization of aromatic amino acids in aqueous solutions. A spin-trapping, and electron spin resonance study. J Phys Chem 1982;86(17):3478–3483.
41. Janzen EG. Spin trapping. Acc Chem Res 1971;4(1):31–40.
42. Symons MCR. Dibromonitroso benzene sulphonate spin-adducts - Why no hyperfine coupling to bromine? Free Radic Res 2000;32(1):25 –29. [PubMed: 10625214]
43. Sanchez-Prado L, Llompart M, Lores M, Garcia-Jares C, Cela R. Investigation of photodegradation products generated after UV-irradiation of five polybrominated diphenyl ethers using photo solid-phase microextraction. J Chromatogr A 2005;1071(1–2):85–92. [PubMed: 15865178]
44. Chignell CF. Spin trapping studies of photochemical reactions. Pure & Appl Chem 1990;62(2):301–305.
45. Wagner BA, Buettner GR, Burns CP. Free radical-mediated lipid peroxidation in cells: Oxidizability is a function of cell lipid bis-allylic hydrogen content. Biochemistry 1994;33(15):4449–53. [PubMed: 8161499]
46. Laarhoven LJJ, Mulder P. α-C-H bond strengths in Tetralin and THF: application of competition experiments in photoacoustic calorimetry. J Phys Chem B 1997;101(1):73–77.
47. Herreno-Sáenz D, Xia Q, Chiu L, Fu P. UVA photoirradiation of halogenated-polycyclic aromatic hydrocarbons leading to induction of lipid peroxidation. Int J Environ Res Public Health 2006;3(2):191–195. [PubMed: 16823092]
48. Akitomo Y, Akamatsu H, Okano Y, Masaki H, Horio T. Effects of UV irradiation on the sebaceous gland and sebum secretion in hamsters. J Dermatol Sci 2003;31(2):151–159. [PubMed: 12670726]
49. Picardo M, Zompetta C, Luca C, Cirone M, Faggioni A, Nazzaro-Porro M, Passi S, Prota G. Role of skin surface lipids in UV-induced epidermal cell changes. Arch Dermatol Res 1991;283(3):191–197. [PubMed: 1867482]

50. Staskal DF, Diliberto JJ, DeVito MJ, Birnbaum LS. Toxicokinetics of BDE 47 in female mice: effect of dose, route of exposure, and time. Toxicol Sci 2005;83(2):215–23. [PubMed: 15509665]

51. Staskal DF, Hakk H, Bauer D, Diliberto JJ, Birnbaum LS. Toxicokinetics of polybrominated diphenyl ether congeners 47, 99, 100, and 153 in mice. Toxicol Sci 2006;94(1):28–37. [PubMed: 16936226]

52. Mazzuckelli LF, Schulte PA. Notification of workers about an excess of malignant melanoma: a case study. Am J Ind Med 1993;23(1):85–91. [PubMed: 8422064]

53. Stapleton HM, Dodder NG, Offenberg JH, Schantz MM, Wise SA. Polybrominated Diphenyl Ethers in House Dust and Clothes Dryer Lint. Environ Sci Technol 2005;39(4):925–931. [PubMed: 15773463]

54. Mancini AJ. Skin. Pediatrics 2004;113(4 Suppl):1114–9. [PubMed: 15060207]

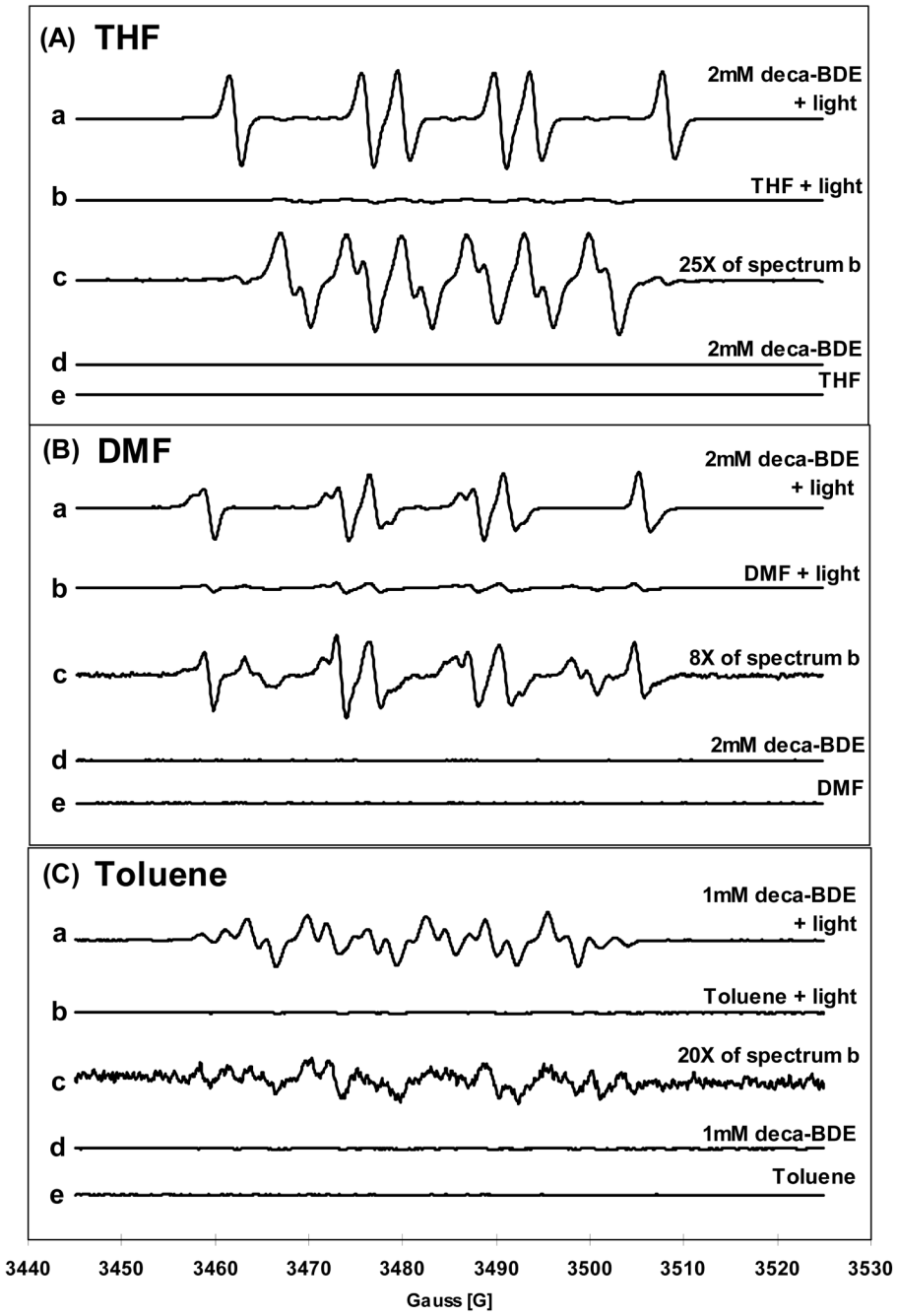

Figure 1. Irradiation of deca-BDE produces free radicals as seen by EPR spin trapping with DMPO

Deca-BDE was dissolved in **(A)** THF with BHT, **(B)** DMF, or **(C)** toluene. a: deca-BDE + light; b: solvent alone + light; c: spectrum b amplified by the factor shown; for example, 25X implies the experimental intensities were multiplied by 25 for display.; d and e: controls without light. The concentration of spin adducts in spectrum (A)-a is approximately 10×10^{-6} M, using 3-CxP as a standard (26).

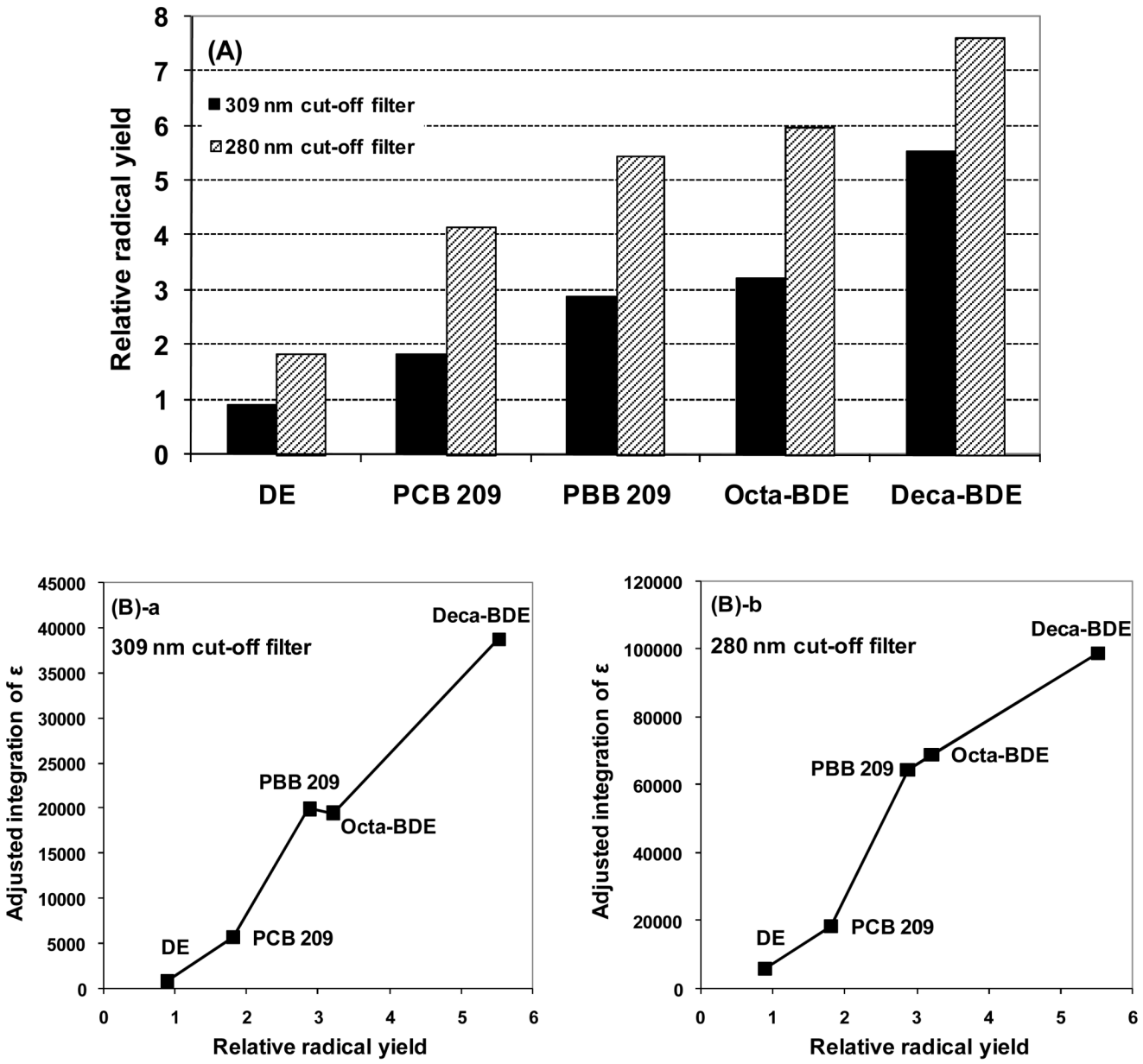

Figure 2. Radical formation by structurally related compounds, relation to UV molar absorption coefficient (ε)

(A) radical yield after irradiation with a 309 nm cut-off filter (black bars) or a 280 nm cut-off filter (striped bars). The radical yield was obtained by double-integration of EPR spectra; relative radical yield: ratio of radical yield of each compound to radical yield of THF alone. **(B)** Radical yield correlated to UV absorption: the area under the absorption curve (ε) was determined by a Trapezoid integration; to estimate the actual light absorbed by the sample when employing a cutoff filter, an "adjusted-integration" was determined by the percent transmittance of the cutoff filter at a specific wavelength times the extinction coefficient of the compound at that wavelength in the integration. **(a)** 309 nm cut-off filter; **(b)** 280 nm cut-off filter.

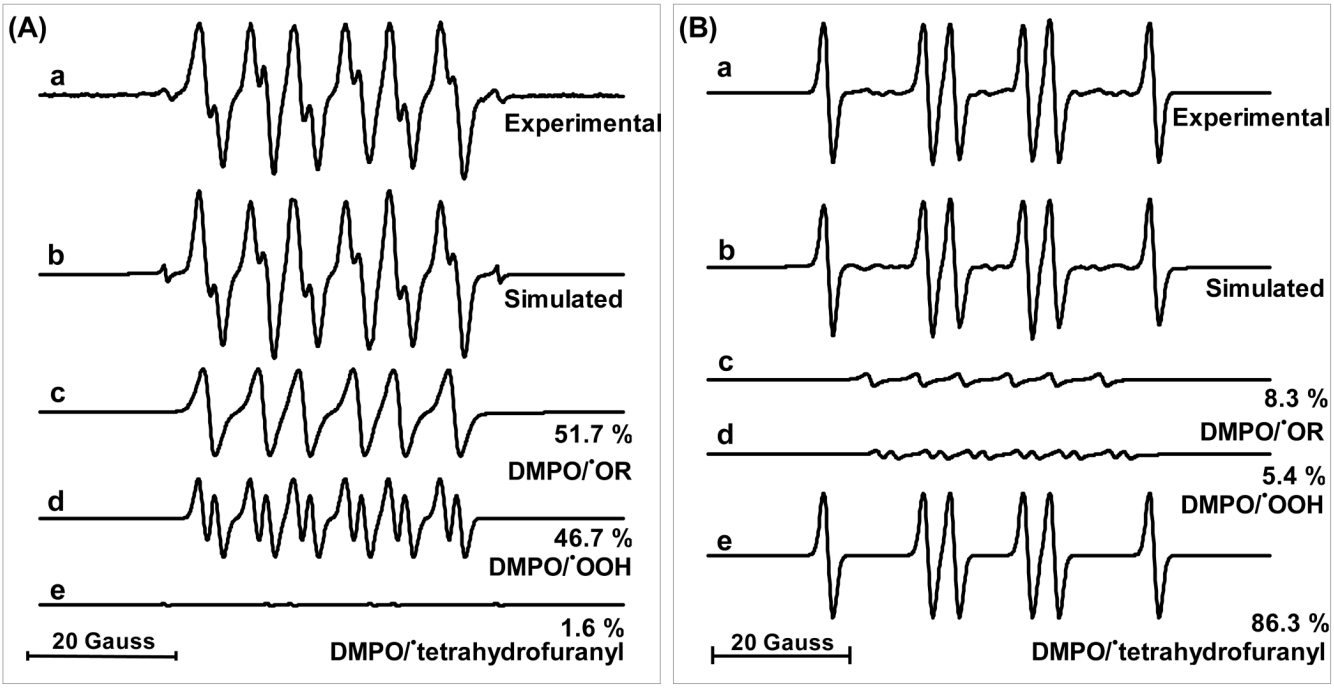

Figure 3. Computer simulations of EPR spectra of DMPO spin adducts in (A) THF with BHT alone, (B) with deca-BDE

(a.) Experimental spectrum; (b.) Composite computer-simulated spectrum; (c.) component of a. corresponding to DMPO/•OR adduct (d.) component of a. corresponding to a DMPO/•OOH adduct (e.) component of a. corresponding to a DMPO/•tetrahydrofuranyl adduct. See Supplement for hyperfine splitting constants.

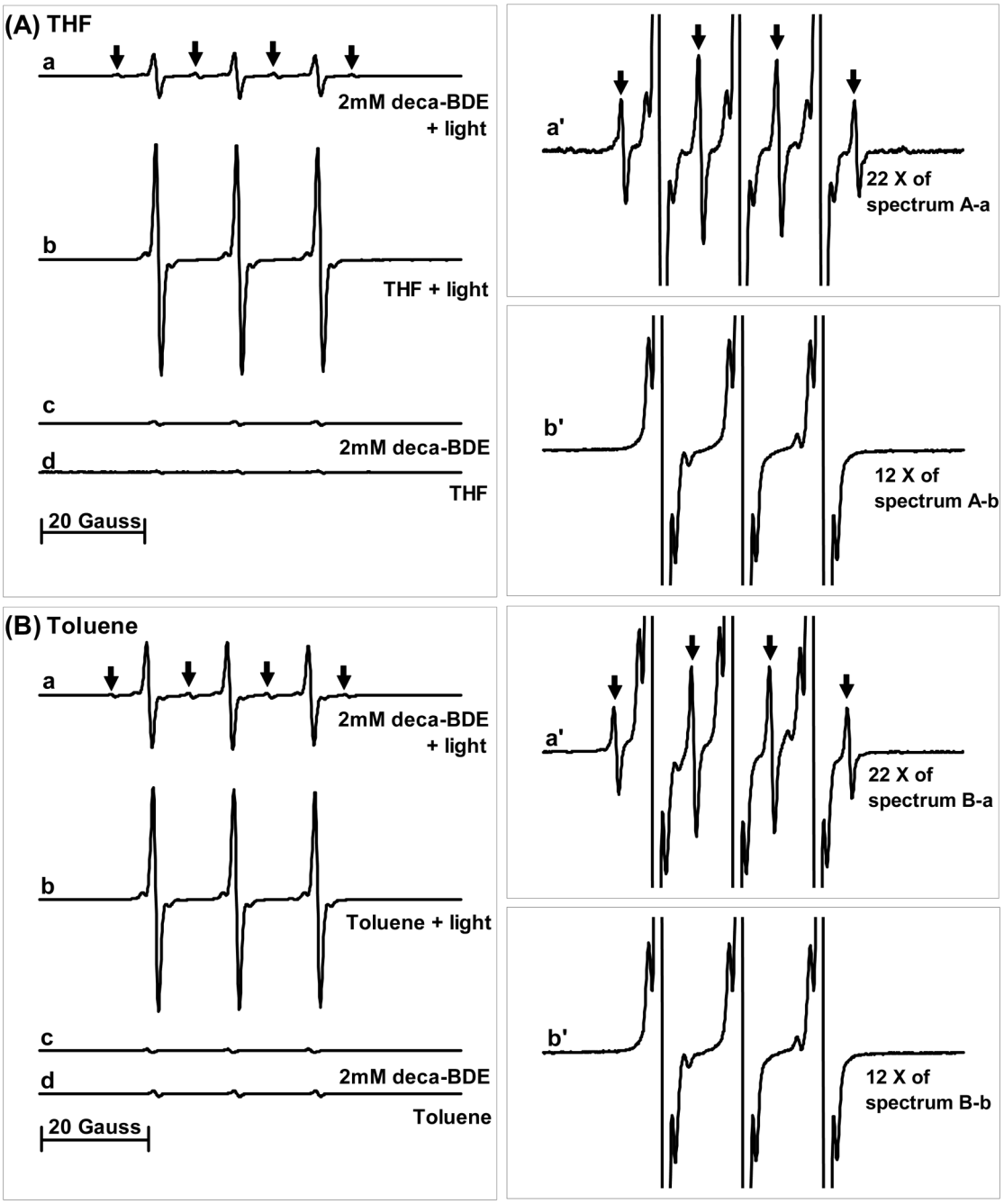

Figure 4. EPR spectra produced by MNP adducts in (A) THF, (B) toluene

(a) deca-BDE + light; (b) solvent alone + light; (a′/b′) is spectrum a/b amplified by the factor shown; (c) and (d) controls with no light. Arrows indicate 1:2:2:1 spectral pattern consistent for the hydrogen (or e^{-}_{aq}, H^{+}) spin adduct of MNP (MNP/$H^{\bullet}$).

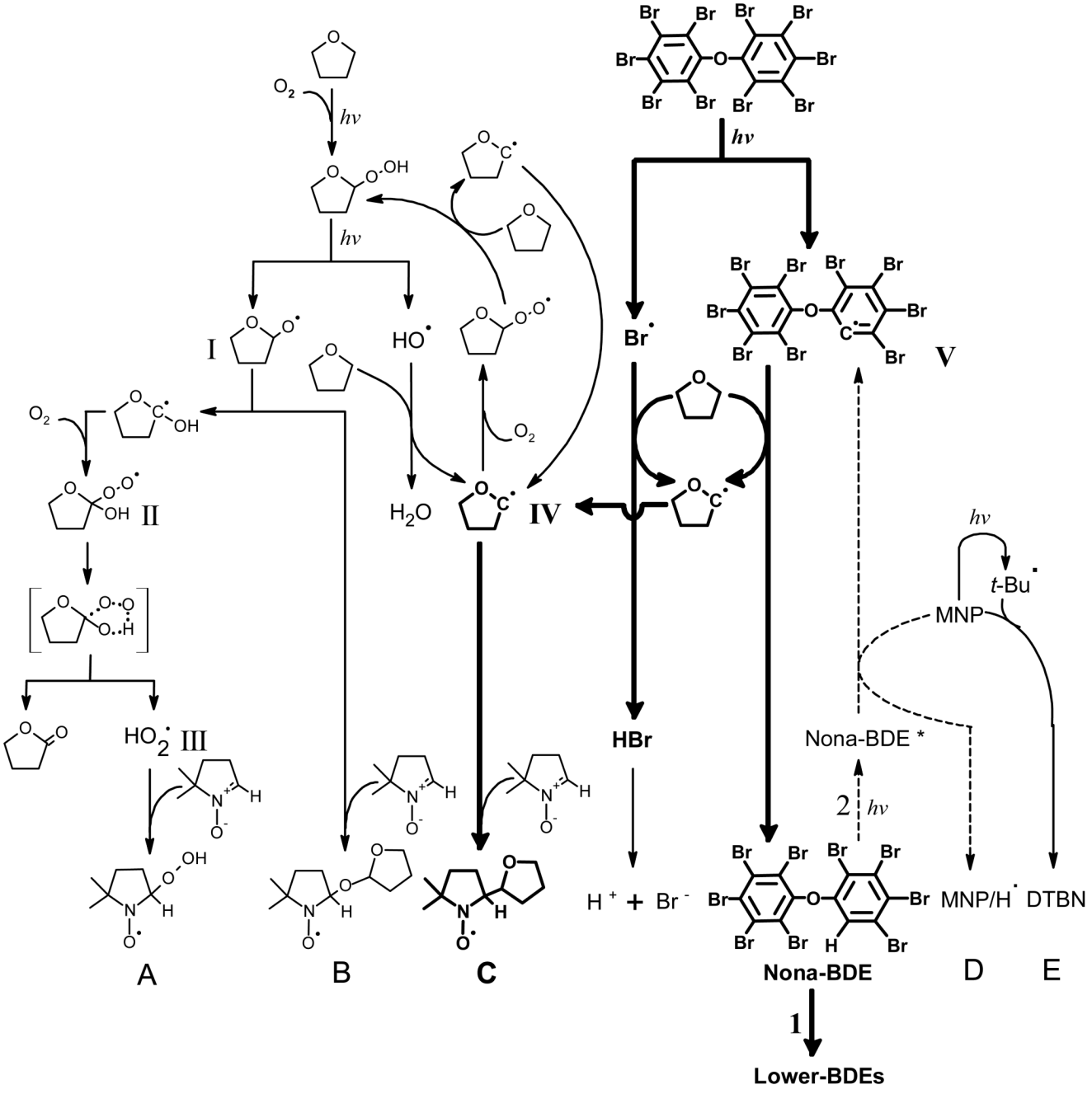

Figure 5. Proposed mechanism of radical formation during irradiation of the deca-BDE in THF

I. Oxygenated tetrahydrofuranyl radical. II. Tetrahydrofuranylhydroperoxyl radical. III. Hydroperoxyl radical. IV. Tetrahydrofuranyl radical. V. Nona-BDE radical. A. DMPO/•OOH. B. DMPO/•OR. C. DMPO/•tetrahydrofuranyl. D. MNP/H•. E. MNP/*tert*-butyl• (DTBN). [] indicates the transition state of II. Nona-BDE* is the excited state of the compound. For nona-BDE pathway 1 is major and 2 (broken arrow) is minor for further reaction.